





 Open access • Posted Content • DOI:10.1101/2020.02.09.940585

## **Correlation network analysis based on untargeted LC-MS profiles of cocoa reveals processing stage and origin country — [Source link](#)**

[Santhust Kumar](#), [Roy N. Dsouza](#), [Marcello Corno](#), [Matthias S. Ullrich](#) ...+2 more authors

**Institutions:** [Jacobs University Bremen](#)

**Published on:** 10 Feb 2020 - [bioRxiv](#) (Cold Spring Harbor Laboratory)

Share this paper:    

View more about this paper here: <https://typeset.io/papers/correlation-network-analysis-based-on-untargeted-lc-ms-345dsv4fij>

1 **Correlation network analysis based on untargeted LC-MS**  
2 **profiles of cocoa reveals processing stage and origin country**

3

4 Santhust Kumar,<sup>1\*</sup> Roy N. D'Souza,<sup>1</sup> Marcello Corno,<sup>2</sup> Matthias S. Ullrich,<sup>1</sup> Nikolai Kuhnert<sup>1</sup>  
5 and Marc-Thorsten Hütt<sup>1\*</sup>

6

7 <sup>1</sup>Department of Life Sciences and Chemistry, Jacobs University Bremen, Campus Ring 1,  
8 28759 Bremen, Germany

9 <sup>2</sup>Barry Callebaut AG, Westpark, Pflingstweidstrasse 60, Zurich 8005, Switzerland

10

11

12 \*Correspondence to:

13 Dr. Santhust Kumar ([s.santhust@jacobs-university.de](mailto:s.santhust@jacobs-university.de))

14 Prof. Dr. Marc-Thorsten Hütt ([m.huett@jacobs-university.de](mailto:m.huett@jacobs-university.de))

15 Department of Life Sciences & Chemistry

16 Jacobs University Bremen gGmbH

17 Campus Ring 1

18 28759 Bremen, Germany

19

20 ABSTRACT

21 In order to implement quality control measures and create fine flavor products, an important  
22 objective in cocoa processing industry is to realize standards for characterization of cocoa raw  
23 materials, intermediate and finished products with respect to their processing stages and  
24 countries of origin. Towards this end, various works have studied separability or  
25 distinguishability of cocoa samples belonging to various processing stages in a typical cocoa  
26 processing pipeline or to different origins. Limited amount of success has been possible in this  
27 direction in that unfermented and fermented cocoa samples have been shown to group into  
28 separate clusters in PCA. However, a clear clustering with respect to the country of origin has  
29 remained elusive. In this work we suggest an alternative approach to this problem through the  
30 framework of correlation networks. For 140 cocoa samples belonging to eight countries and  
31 three progressive stages in a typical cocoa processing pipeline we compute pairwise Spearman  
32 and Pearson correlation coefficients based on the LC-MS profiles and derive correlation  
33 networks by retaining only correlations higher than a threshold. Progressively increasing this  
34 threshold reveals, first, processing stage (or sample type) modules (or network clusters) at low  
35 and intermediate values of correlation threshold and then country specific modules at high  
36 correlation thresholds. We present both qualitative and quantitative evidence through network  
37 visualization and node connectivity statistics. Besides demonstrating separability of the two  
38 data properties via this network-based method, our work suggests a new approach for studying  
39 classification of cocoa samples with nested attributes of processing stage sample types and  
40 country of origin along with possibility of including additional factors, e.g., hybrid variety, etc.  
41 in the analysis.

42

43 **Keywords:** *Theobroma cacao*, LC-MS, correlation network, origin classification, processing-  
44 stage classification.

45

## 46 **1. Introduction**

47 Cocoa, scientifically *Theobroma cacao*, is a commodity of commercial interest to farmers as a  
48 crop and to businesses as a raw material for producing various cocoa based food products.  
49 Therefore, quality, variety and characteristics of cocoa and its derived food items have become  
50 an important area of research and development. Quality control (Fayeulle et al., 2019; Guehi  
51 et al., 2010; Kongor et al., 2016; Lima et al., 2011) and design of single origin cocoa products  
52 (Oberrauter et al., 2018; Ozretic-Dosen et al., 2007) are two of many focus areas in cocoa  
53 research. The former helps in ensuring whether the stages in a typical cocoa processing pipeline  
54 have been rightly carried to achieve the best possible finished product, and the latter commands  
55 high value among consumers for nuanced taste and aroma of the consumed food item.

56 Previous research successfully demonstrate characteristic differences between unfermented,  
57 partially fermented and fermented cocoa samples (processing-stages) and even identified  
58 corresponding potentially responsible classes of compounds through multivariate statistical  
59 analysis, e.g., principal component analysis (PCA) (Wold et al., 1987), on the chemical  
60 composition of these samples (Caligiani et al., 2014; D'Souza et al., 2017; Kumari et al., 2018;  
61 Megías-Pérez et al., 2018). Baring a few cases where the number of distinct countries relating  
62 to the samples in dataset at hand is few (D'Souza et al., 2017; Milev et al., 2014; Oliveira et  
63 al., 2016) or based on large continental regions (Acierno et al., 2016, 2018; Bertoldi et al.,  
64 2016; Kumari et al., 2018; Marseglia et al., 2016), a successful characteristic differentiation  
65 amongst samples on the basis of their country of origin has remained hard to define through  
66 metabolomic analysis (D'Souza et al., 2017; Sirbu et al., 2018; Vázquez-Ovando et al., 2015).

67 On the other hand, the 'language of networks' (Albert and Barabási, 2002; Newman, 2003) has  
68 proven immensely useful in visualizing and interpreting relationships between multitude of  
69 entities, and across many disciplines—metabolomics (Jeong et al., 2000), genetics (Grimbs et

70 al., 2019; Kumar et al., 2018), proteomics (Szkarczyk et al., 2015), social science (Borgatti et  
71 al., 2009), logistics (Becker et al., 2012), gut ecology (Claussen et al., 2017) medicine  
72 (Barabási et al., 2011; Batushansky et al., 2016), finance (Kumar and Deo, 2012; Namaki et  
73 al., 2011), etc. to name a few. Some works have successfully applied this approach in the field  
74 of food science (Ahn et al., 2011; Hochberg et al., 2013; Ursem et al., 2008; Wang et al., 2017).

75 Here, we apply the framework of network science to simultaneously study the clustering of  
76 cocoa samples with regards to their processing-stage sample types and country of origin.

77 We start by computing pairwise Spearman and Pearson correlation coefficients between 140  
78 cocoa samples belonging to three different stages in a typical cocoa processing pipeline  
79 (unfermented, fermented and liquor) and 8 countries through their LC-MS profiles in positive  
80 ion mode. On the basis of correlations obtained, we construct correlation networks, at varying  
81 correlation thresholds. In these networks, the nodes are samples and an edge between two  
82 samples is drawn, when the correlation coefficient exceeds the threshold value.

83 We find that, as we progressively increase the correlation threshold from 0 towards 1, the  
84 clustering of cocoa samples is first dominated by processing-stage sample types at low and  
85 intermediate correlation thresholds, and then by countries of origin at high correlation  
86 thresholds. We show this both qualitatively and quantitatively via network visualizations and  
87 network edge statistics.

88 Our work demonstrates the presence of processing-stage level grouping on a coarser level and  
89 origin level grouping on a finer level within the former. This nested grouping can be revealed  
90 by successively keeping higher correlations. Further, our works suggests a new approach to  
91 study clustering or classification of food samples upon multiple nested attributes and can prove  
92 an important complement to traditional approaches and strategies.

93

## 94 2. Materials and Methods

### 95 2.1 Country and Origin details

96 The LC-MS data set we use here has a total of 140 samples (positive ion mode). The samples  
97 have been gathered and their LC-MS profiling done under COMETA project over a range of  
98 about past five years. These samples can be grouped into three sample-types (Unfermented,  
99 Fermented and Liquors) and eight origins (Brazil, Cameroon, Ecuador, Ghana, Indonesia,  
100 Ivory Coast, Malaysia and Tanzania). A cross-table of details about number of samples  
101 belonging to particular sample-type and country is given in Table 1.

102

103

	Brazil	Cameroon	Ecuador	Ghana	Indonesia	Ivory coast	Malaysia	Tanzania	All
<b>Unfermented</b>	4	3	8	0	14	16	6	3	<b>54</b>
<b>Fermented</b>	4	3	12	0	16	16	3	9	<b>63</b>
<b>Liquor</b>	0	6	3	5	0	9	0	0	<b>23</b>
<b>All</b>	<b>8</b>	<b>12</b>	<b>23</b>	<b>5</b>	<b>30</b>	<b>41</b>	<b>9</b>	<b>12</b>	<b>140</b>

104 **Table 1 Sample division.** The LCMS data set can be grouped on twin axes: sample-type and  
105 origin. There are 3 sample-types: Unfermented, Fermented and Liquors, and there are 8 origins  
106 (Brazil, Cameroon, Ecuador, Ghana, Indonesia, Ivory Coast, Malaysia and Tanzania).

### 107 2.2 Data pre-processing and cleaning

108 The data generation, cleaning, standardization and organization has been discussed in an earlier  
109 work (Kumar et al *previous manuscript*). Briefly, LC-MS data of all the samples was processed

110 using MZMine (Pluskal et al., 2010) giving peak area list and corresponding *m/z ratio* and  
111 *retention times*. The detected compounds are assigned names/chemical formula on the basis of  
112 four ionization states ([M+H], [M+2H], [M+3H], [2M+H]) when possible, else the compound  
113 was named as ‘Unknown\_’ suffixed with the *m/z* value, e.g., Unknown\_865.1927. The samples  
114 were then put in an excel file, where each row represents a sample, and the column contain  
115 information about the sample-type, origin and peak areas of various compounds sorted in  
116 descending order by their mean peak are across all the samples.

### 117 **2.3 Network production and visualization**

118 Spearman and Pearson correlation analysis, and network generation/transformation was carried  
119 by writing programs from scratch in Python programming language making use of popular  
120 modules such as Pandas (McKinney, 2010, 2011) and NetworkX (Hagberg et al., 2008).  
121 Network visualization has been done in Cytoscape (Shannon et al., 2003). For layout of the  
122 network either of the following two variants of spring layout, which were available in  
123 Cytoscape itself, were used: (a) Edge-weighted Spring Embedded Layout (Kamada and Kawai,  
124 1989), (b) Compound Spring Embedder (CoSE) (Dogrusoz et al., 2009). These layouts take  
125 into account the weight of the edge (in our case the Spearman or Pearson correlation  
126 coefficient) between nodes, so that the nodes with higher weight (correlations) are placed closer  
127 together.

### 128 **2.4 Null model network or control network**

129 A null model network is made by randomizing the weights (correlations) of edges in the  
130 original correlation network. It is important to note that the null model network so obtained has  
131 the same correlation distribution as that of the original correlation network because the set of  
132 correlations in the network remains unchanged, only the correlations between nodes is  
133 randomized. An ensemble of 100 such null model networks were generated. The reported



134 statistics about a studied property on the null model networks is obtained by making  
135 calculations over this ensemble and then reporting the mean and standard deviation of the  
136 studied property. Higher the difference in the studied property between the original network  
137 and null network ensemble, higher the significance of the observed property in the original  
138 network.

### 139 **3. Results**

#### 140 **3.1 Correlation between cocoa samples**

141 A typical LC-MS profile contains information about thousands of compounds present in a  
142 given sample defined by their retention time and associated  $m/z$  values (Kuhnert et al., 2013).  
143 Using the areas of peaks as a rough measure for concentration of these compounds across all  
144 samples, we calculate the Spearman and Pearson correlation coefficients ( $r$ ) for all pairs of  
145 samples in our dataset.

146 The LC-MS data can be represented as a matrix  $L$  with entries  $l_i^\alpha$ . The upper index  $\alpha$  represents  
147 the sample and lower index  $i$  represents the compound. Thus, the scalar quantity  $l_i^\alpha$  represents  
148 the concentration of  $i^{\text{th}}$  compound in the  $\alpha^{\text{th}}$  LC-MS sample. Correspondingly,  $l^\alpha$  is a vector  
149 which represents the LC-MS profile of sample  $\alpha$ . The Pearson correlation between two LC-  
150 MS samples, say  $\alpha$  and  $\beta$  with corresponding profiles  $l^\alpha$  and  $l^\beta$ , can be denoted as  $r_{\alpha\beta}$ . It is  
151 calculated as

$$152 \quad r_{\alpha\beta} = \frac{\text{cov}(l^\alpha, l^\beta)}{\sigma_{l^\alpha} \sigma_{l^\beta}}$$

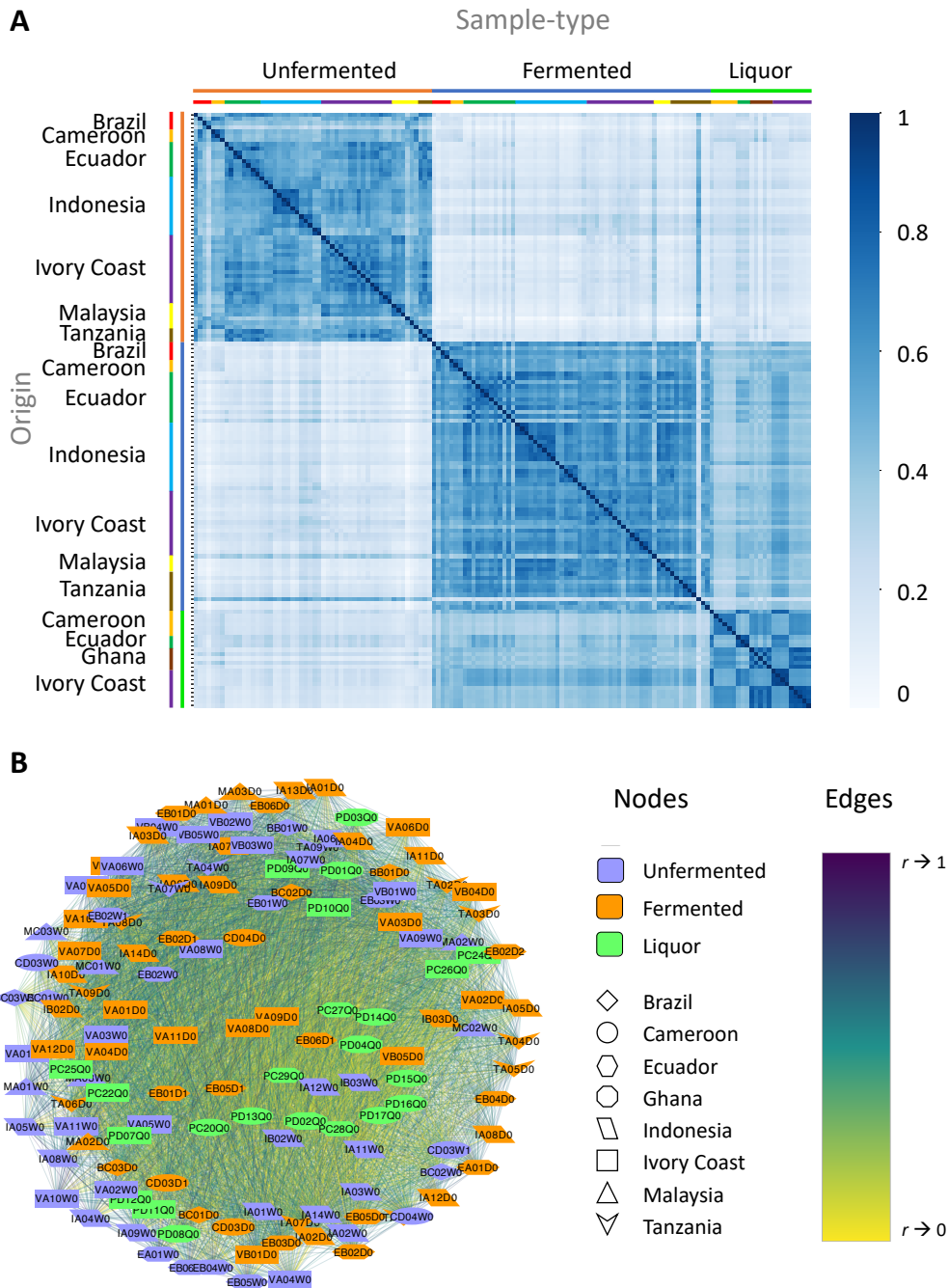
153 Where  $\text{cov}(l^\alpha, l^\beta)$  represents the covariance between the LC-MS profiles of samples  $\alpha$  and  $\beta$ ,  
154 while  $\sigma_{l^\alpha}$  and  $\sigma_{l^\beta}$  represent the standard deviation in the LC-MS profiles  $l^\alpha$  and  $l^\beta$ ,  
155 respectively. The Spearman correlation can be defined as the Pearson correlation between the

156 ranks of the original variables (i.e.,  $l^\alpha$  and  $l^\beta$ ). The ranked variables  $\tilde{l}^\alpha$  and  $\tilde{l}^\beta$ , are obtained  
157 from the original variables  $l^\alpha$  and  $l^\beta$  by sorting them from lowest to highest and substituting  
158 the values by the position in the sorted list (i.e., the rank of the values). Formally, the Spearman  
159 correlation coefficient is thus calculated as

$$160 \quad \tilde{r}_{\alpha\beta} = \frac{\text{cov}(\tilde{l}^\alpha, \tilde{l}^\beta)}{\sigma_{\tilde{l}^\alpha} \sigma_{\tilde{l}^\beta}}$$

161 The Spearman and Pearson correlations across all pairs of LC-MS samples can be written in  
162 the form of matrices,  $\tilde{R}$  and  $R$ , whose entries denoted by  $\tilde{r}_{\alpha\beta}$  and  $r_{\alpha\beta}$ , respectively.

163 The correlation matrices  $\tilde{R}$  so obtained, i.e. the case of Spearman correlation coefficient, is  
164 visualized through heatmap in Figure 1A. The heat map of Pearson correlation coefficient  
165 matrix,  $R$ , is given in Supplementary Information file. By construction the correlation matrices  
166  $\tilde{R}$  and  $R$  are symmetric. The twin attributes of nodes, namely the processing-stage sample type  
167 and country of origin, have been alternatively marked on the sides. Three blocks corresponding  
168 to Unfermented, Fermented and Liquor samples blocks are clearly distinguishable. It is also  
169 visible that Fermented and Liquor samples are part of a larger block which is separated from  
170 Unfermented samples. This shows that Liquor samples are closer in character to Fermented  
171 samples. This is in consonance with general expectation that liquor follows the fermentation  
172 stage. Furthermore, more chemical changes occur in cocoa when moving from unfermented  
173 stage to fermented stage than occurs from fermented to liquor stage. In case of correlation  
174 heatmap obtained using Pearson correlation (Supplementary Information file) the block of  
175 Unfermented samples is clearly distinguishable from Fermented and Liquor samples, while the  
176 Fermented and Liquor samples are mildly distinguishable. Further, it is important to note that  
177 no block structure on the basis of country is discernable at this level of detail about the  
178 correlations.



179

180

181

182

183

184

185

**Figure 1 Correlation between cocoa samples.** (A) Correlation heatmap. Darker regions represent high correlation, and lighter regions represent low correlation. Samples have been sorted on twin axes, first on processing stage sample-type, and then second internally on country of origin. Two distinct square block regions are clearly visible along the diagonal of the matrix, corresponding to Unfermented (smaller block) and Fermented (bigger block) samples. (B) Correlation Network. The correlation network made using all correlations between the set of

186 cocoa samples using Spearman correlation. The nodes are color coded according to their  
187 processing-stage sample type and shape coded by their country of origin. The colors of edges  
188 code for the strength of correlation between nodes. The network is visualized using Cytoscape  
189 (Shannon et al., 2003) with ‘edge-weighted spring embedded layout’ which keeps nodes  
190 connected with higher correlations closer together.

191

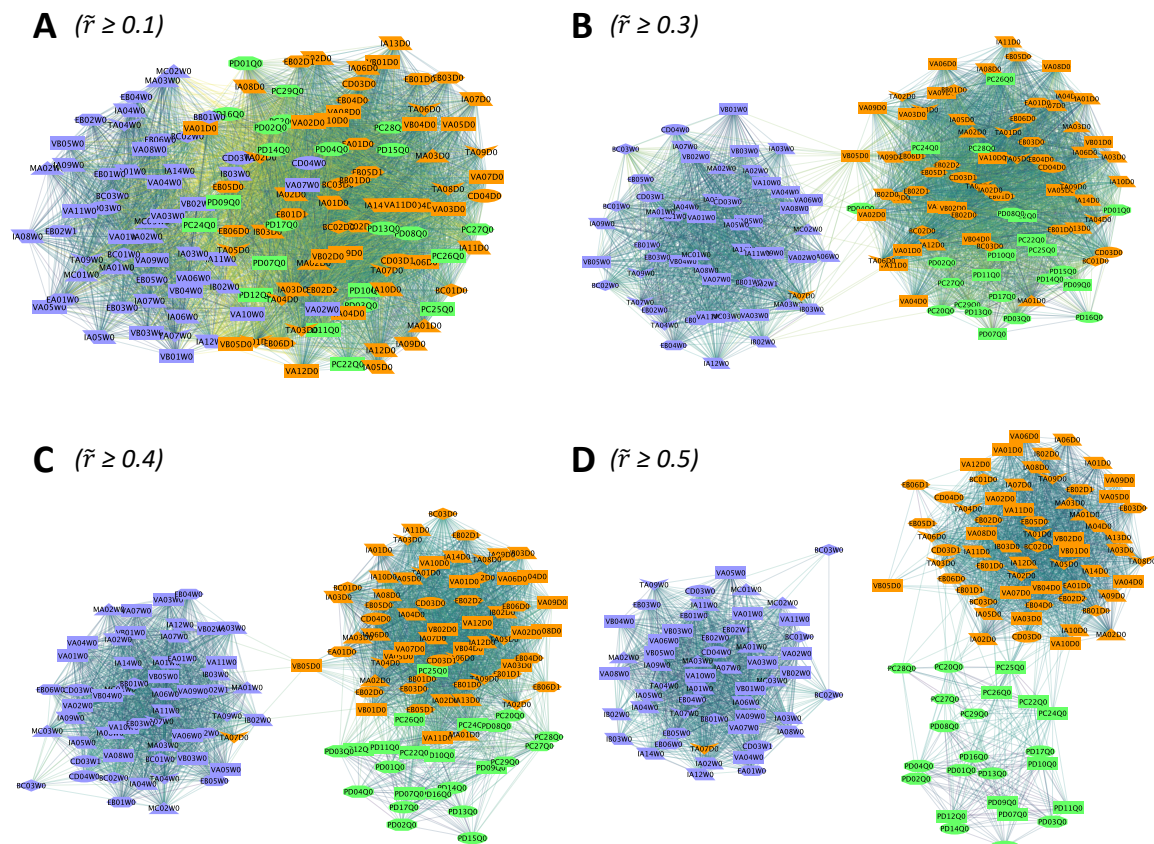
192 Next, we define correlation network using the Spearman ( $\tilde{r}$ ) and Pearson correlations ( $r$ )  
193 obtained above. A network is defined through two sets of entities: nodes ( $N$ ) and edges ( $E$ ).  
194 The nodes denote the objects which are related to each other in some way, and the edge  
195 represent the relation between the nodes. For further knowledge about network, see (Albert and  
196 Barabási, 2002; Newman, 2003). In a correlation network, an edge represents the correlation  
197 between two nodes. In our correlation network, the nodes represent the different LC-MS  
198 samples of cocoa or its products sourced from different origins, and the edge between the nodes  
199 represent the correlation between the LC-MS samples. Figure 1B shows the correlation  
200 network obtained by using all correlations (0 to 1) between all LC-MS samples and visualized  
201 with edge-weighted spring layout (see section 2.3 Network production and visualization).  
202 Metadata about the LC-MS samples, such as country, and processing-stage sample type  
203 (unfermented, fermented, or liquor) has been represented through color and shape of nodes,  
204 respectively. The network shown in Figure 1B is the correlation network made using Spearman  
205 correlation and has 140 nodes and 6833 edges, i.e. 140 cocoa LC-MS samples and 6833  
206 correlations ( $\tilde{r} > 0$ ) between the nodes. The network made using Pearson correlation is shown  
207 in the Supplementary Information file. The label of the node represents the internal LC-MS id.  
208 The strength of correlation is represented by the color of the edge between the nodes, yellow  
209 representing low correlation and violet representing high correlation. The spatial placement of  
210 nodes in Figure 1B, and all of the following networks, is done through variants of spring layout

211 algorithms in Cytoscape (Shannon et al., 2003) which places the nodes with higher correlation  
212 closer together (2.3 Network production and visualization).

### 213 **3.2 Networks at low and intermediate correlation thresholds reveals processing-stage** 214 **sample type modules**

215 Next, we analyze correlation networks at low and intermediate correlation thresholds ( $\tilde{r}_{th}$ ),  
216 varying it from  $\tilde{r}_{th} = 0.1$  to 0.5, in steps of 0.1. The network at a given correlation threshold  
217 contains all the edges with correlation greater than or equal to the set threshold. Some of these  
218 networks are visualized in Figure 2. Panels A, B, C and D in Figure 2 show the network at  
219 correlation thresholds of 0.1, 0.3, 0.4 and 0.5, respectively. In panel A, the nodes belonging to  
220 Unfermented samples are seen little separated from the nodes belonging to the Fermented and  
221 Liquor samples. In panel B, the Unfermented samples are clearly separated from the Fermented  
222 and Liquor samples. Within the Fermented and Liquor samples little grouping starts to form.  
223 In panel C, the separation between the Fermented and Liquor samples becomes enough clear.  
224 And in panel D, all the three samples can be seen clearly separated from one another. This  
225 separation of samples first into two groups: (a) Unfermented, and (b) Fermented and Liquor  
226 samples, and then slowly into three groups: Unfermented, Fermented and Liquor samples, is  
227 in congruence with the earlier result seen in the structure of the correlation matrix heatmap  
228 shown in Figure 1A. Both Figure 1A and Figure 2B,C show that the liquor sample are more  
229 similar to the fermented samples than to the unfermented samples. This is in accordance with  
230 the fact that major chemical and physical changes in cocoa beans takes place during the  
231 processes of fermentation. A movie of the network as a function of progressively increasing  
232 the threshold is attached as supplementary information which clearly shows the evolving  
233 network and separation of samples belonging to different cocoa processing stage. Similar  
234 behavior is noted for the case of correlation network formed using the Pearson correlation

235 coefficient (Supplementary Information file) however at different values of correlation  
236 threshold.



237

238 **Figure 2 Processing-stage modules in low and intermediate threshold correlation**

239 **networks.** The figure reveals modules of samples belonging to the same cocoa processing-stage

240 in a typical cocoa processing pipeline. **(A)** Network of LC-MS samples at a correlation threshold

241 of 0.1 revealing separation of unfermented, fermented and liquor cluster. **(B, C)** Correlation

242 thresholds 0.3 and 0.4. The separation between different processing-stage sample types

243 improves. **(D)** Correlation threshold 0.5. Three groups of unfermented, fermented and liquor

244 samples are clearly separated. The figure follows same legend as of Figure 1

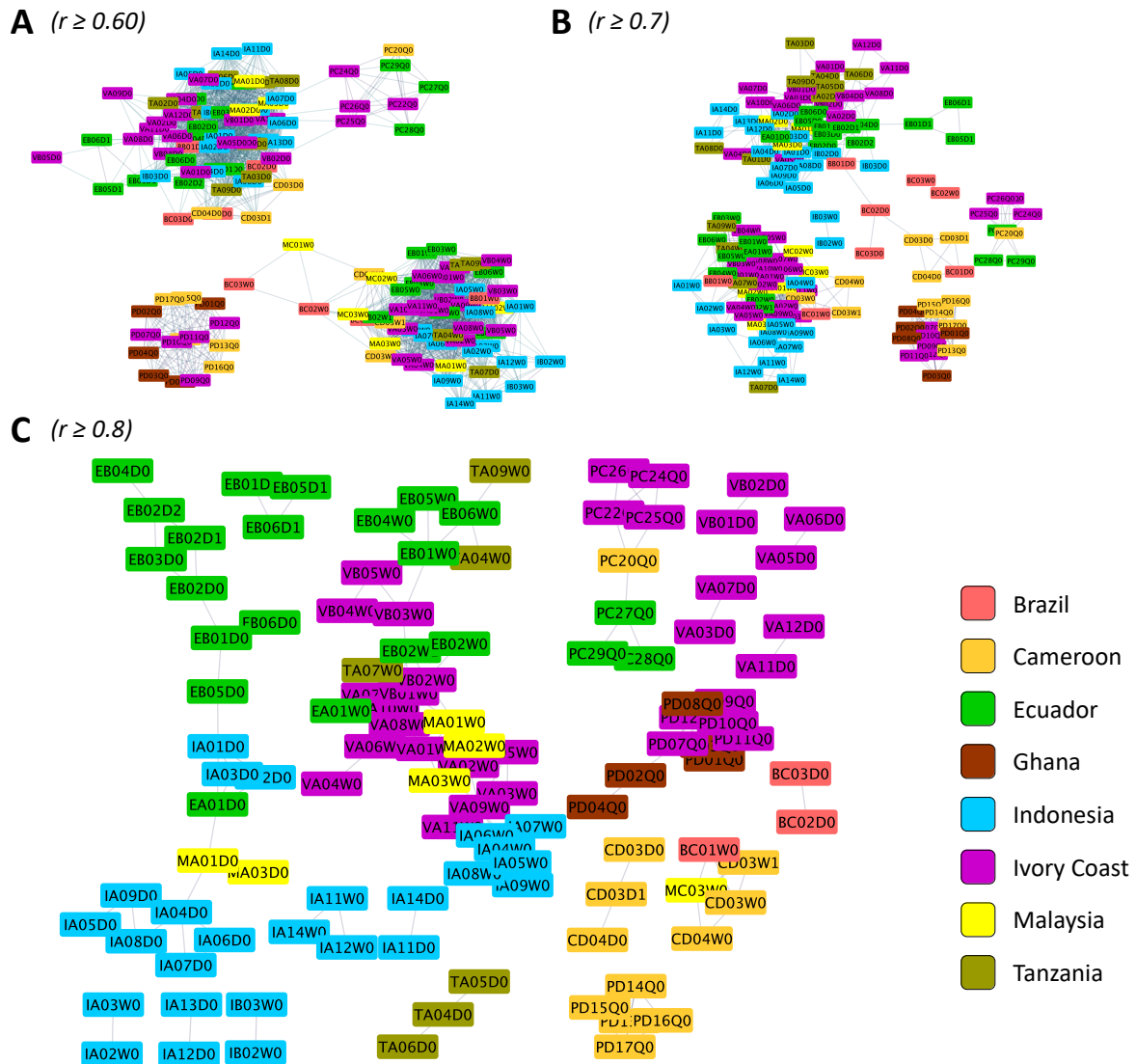
245 **Error! Reference source not found..** See supplementary information for a movie on evolving network as the

246 correlation threshold is progressively increased.

247 **3.4 Country enriched modules at high correlation thresholds**



248 As the correlation threshold is further increased, the network breaks into various smaller  
249 connected components. The resulting individual connected components primarily have the  
250 processing-stage sample type. However, there are more than one component that belong to  
251 same color or sample type. This reveals the internal structure of the clusters of samples that  
252 initially grouped on the basis of their sample types. This additional sub-structure of the network  
253 reveals grouping which now is primarily governed by the samples belonging to same country  
254 of origin. This is shown in the networks in Figure 3 for correlation thresholds of 0.6, 0.7 and  
255 0.8. Panels A and B provide a bird's-eye view at respective thresholds, while panel C gives a  
256 detailed view. In contrast to the legend used in previous figures, we now color the nodes on the  
257 basis of countries for a quick comprehension of grouping on the basis of countries. The figure  
258 with the previous legend scheme is given as Supplementary Information. It can be seen from  
259 the figure that same color nodes tend to be present closer together. This feature is visible more  
260 in modules of smaller size, but it is also discernible in larger sized modules. We see that as the  
261 correlation threshold is further increased, most of the larger size modules break into smaller  
262 module, where nodes belonging to the same origin country are increasingly often connected. It  
263 should be noted that processing-stage and country of origin are only the major governing  
264 factors, on which grouping of samples is based. Other factors such as variety of cocoa hybrid,  
265 harvest season, geographical location and landscape of farm in the country etc, can begin to  
266 play an important role with increasing correlation threshold. Hence the clustering is not perfect.  
267 The other governing factors can potentially lead to finer sub-modular structures in the network.  
268 This situation is more likely to be evident at still higher correlation thresholds.



269

270

271

272

273

274

275

276

277

278

279

**Figure 3 Country modules.** The structure of correlation network of cocoa samples based on their LCMS profile at correlation thresholds of 0.80, 0.85 and 0.90. At these correlation thresholds, several modules with nodes belonging to the same country of origin are revealed. For a quick and better comprehension and unlike the legend of earlier correlation networks, in this figure different countries are represented through a different color. The networks with same thresholds but with previous annotation (i.e. of Figure 1 and Figure 2) is given in Supplementary Information for comparison. See supplementary information for a movie on evolving network as the correlation threshold is progressively increased.

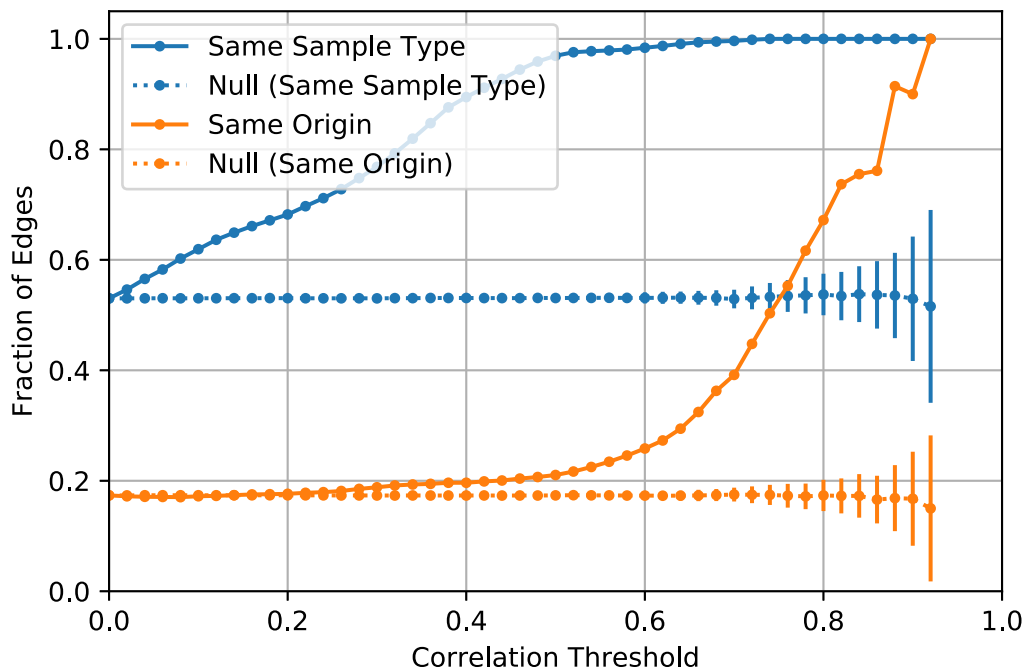


280 As the correlation threshold is gradually increased, edges with correlation less than the  
281 threshold value are lost from the network. On one hand this leads to increased consideration of  
282 the edges with higher correlation in the determination of the layout of the network, while on  
283 the other this, naturally, leads to decrease in the number of edges, and when possible, also  
284 decreases the number of nodes in the resulting network, resulting in network breakage. The  
285 variation of number of edges and number of nodes connecting them is shown in the  
286 Supplementary Information file. In our networks here, only the edges greater than the set  
287 correlation threshold and corresponding nodes are present. A movie of the network as a  
288 function of progressively increasing the threshold is attached as supplementary information  
289 which clearly shows the evolving network and separation of samples belonging to different  
290 countries.

### 291 **3.5 Similarity of nodes connected by an edge**

292 As a node in our correlation networks has two attributes, namely the processing-stage sample-  
293 type and origin, we define two kinds of similarity for a pair of nodes connected by an edge:  
294 sample-type similarity and origin similarity. We define sample-type similarity as the fraction  
295 of edges in a network connecting nodes having the same processing-stage sample-type  
296 attribute, and origin similarity as the fraction of edges in a network connecting nodes which  
297 have same origin attribute. The sample-type and origin similarities as a function of correlation  
298 thresholds based on Spearman correlation networks are shown in Figure 4 (solid lines). They  
299 differ significantly from each other in terms of both the correlation threshold around which  
300 they start to rise and the manner in which they rise. The sample-type similarity starts to increase  
301 right from the smaller values of correlation thresholds itself and in a linear manner until it starts  
302 to saturate around a correlation threshold value of 0.5 to a similarity value close to 1. This is in  
303 agreement with the observed enhancement of the processing-stage sample type character of the

304 network architecture right from the beginning of starting values of correlation threshold, to the  
305 almost full appearance of processing-stage sample type character at intermediate correlation  
306 threshold in large and small connected components (cf. Figure 2). The origin similarity remains  
307 almost constant and close to that of null model networks (orange dashed line) for a long range  
308 of correlation threshold (up to 0.5) suggesting a weak or almost negligible role in the clustering  
309 of nodes belonging to the same origin in the layout of network. Only when the correlation  
310 threshold is around 0.5, origin similarity starts to increase, suggesting this is the value of  
311 correlation threshold at which the contribution of origin effects start to contribute in clustering  
312 of nodes belonging to same origin begins. This clearly shows that the processing-stage sample  
313 type effect precedes the country effects, and the country effects are finer than the sample-type  
314 effect. The origin similarity increases exponentially and reaches a value close to 1. This implies  
315 that at higher threshold almost all edges connect nodes having same sample type and same  
316 country of origin.



317

318 **Figure 4 Connected nodes' similarity.** The sample-type similarity (blue line) starts to increase  
319 linearly right from smaller correlation threshold values, reaches close 1 around a correlation  
320 threshold value of 0.5. The origin similarity remains constant for a long range of correlation  
321 threshold (0, 0.50) and then increases exponentially. The dashed lines show corresponding  
322 similarities as expected from an ensemble of control networks.

323 The dashed lines along with error bars show similarity values and standard deviation expected  
324 from an ensemble of null model networks (control networks) obtained by randomizing edge  
325 weights in the original network (see 2.4 Null model network or control network). The  
326 difference between the similarity values from original network and that obtained null model  
327 networks points to the fact that the networks at higher correlation thresholds are enriched in  
328 edges that have high sample-type and origin similarity. The result corresponding to correlation  
329 network generated using Pearson correlation coefficient is given in Supplementary Information  
330 file. Both show similar behavior, although at slightly different correlation threshold value.

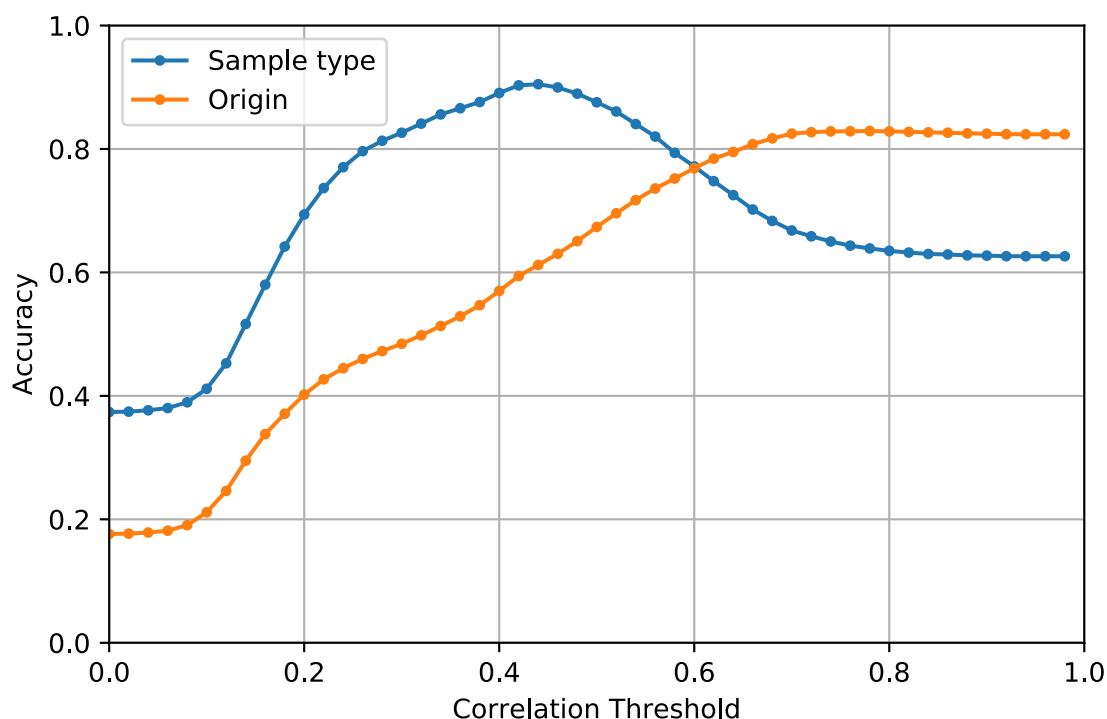
### 331 **3.6 Closeness of thresholded networks to ideal networks**

332 In this section, we quantify as a function of correlation threshold how accurately our networks  
333 represent the expected ideal networks of cocoa samples given their processing-stage sample  
334 types or country of origin. We consider two ideal networks, one each for the processing-stage  
335 sample type and country of origin. An ideal processing-stage sample type based network will  
336 have a link between a pair of its nodes only when both the nodes belong to the same processing-  
337 stage sample type, otherwise the link would be absent. Similarly, an ideal origin-based network  
338 will have a link between a pair of its nodes only when both the nodes belong to the same  
339 country of origin. Thus, in an ideal network based upon processing-stage sample type or  
340 country of origin a link is present only between nodes belonging to same sample type, or nodes  
341 belonging to same origin, otherwise there is no link between dissimilar nodes. After defining  
342 these ideal or true networks, we identify 'true positive' and 'true negative' links by comparing

343 the links in the original network at a given correlation threshold (or thresholded network, for  
344 short) with the links in the ideal networks. A link is counted to be ‘true positive’ when the link  
345 is present both in the original network at the given threshold and the corresponding ideal  
346 network. A link is counted as ‘true negative’ when the link is absent both in the network at the  
347 given threshold and the corresponding ideal network. On the other hand, a link is defined as  
348 ‘false positive’ when it is present in the thresholded network but not in the corresponding true  
349 network, and ‘false negative’ when it is absent in the thresholded network but present the true  
350 network. An illustration of this scheme through a toy network is provided in Supplementary  
351 Information file. Using these terms, we define accuracy  $\alpha$  as the fraction of ‘true positive’ and  
352 ‘true negative’ links in an original thresholded network. Accuracy quantifies how close a  
353 thresholded network is to the ideal expected network.

354 We find that with increasing correlation thresholds the network becomes closer to the expected  
355 true network as demonstrated by increasing values of accuracy for both processing-stage  
356 sample type and country of origin Figure 5 (Spearman correlation network; Pearson correlation  
357 case in Supplementary Information file). Further, in the region of low correlation threshold the  
358 character of the network is closer to that of the expected true network for the processing-stage  
359 sample type attribute, and in the region of higher correlation threshold the character of the  
360 network is closer to that of the expected true network for country of origin attribute. This result  
361 is in agreement with the previous results with formation of processing-stage sample type  
362 clusters at lower and intermediate correlation thresholds and of country-based clusters at high  
363 correlation thresholds.

364



365

366

367

368

369

370

371

372

373

**Figure 5 Accuracy of links in thresholded correlation networks, or closeness of a thresholded correlation network to expected ideal network based on sample type or origin attributes of cocoa samples.** As the correlation threshold increases the threshold networks become closer to their ideal counterparts. In regions of lower correlation threshold, the thresholded networks are describe more the sample type character of the network than the origin type character. In regions of higher correlation threshold, opposite is true and the thresholded networks are closer in their character to the origin attribute of LC-MS samples. This is coherent with the network pictures at various threshold seen in earlier figures.

374

#### 4. Conclusions and Discussion

375

376

377

378

We have introduced a new approach for studying grouping in cocoa samples using their LC-MS profile. This new approach is often called ‘network science’, and it already benefits a multitude of scientific disciplines. Few cases also exist where network approach has been successfully applied in food science for different purposes (Hochberg et al., 2013; Ursem et

379 al., 2008; Wang et al., 2017), however, to the best of our knowledge, we apply it for the first  
380 time to study the classification of cocoa samples based upon their LC-MS profiles.

381 Classification of cocoa samples on the basis of their country of origin has been found  
382 challenging with limited success obtained in cases with the number of countries being few or  
383 the origin being on continental scale. Differences in unfermented and fermented samples can  
384 be easily seen by simply finding the Spearman correlation between the cocoa samples using  
385 their LC-MS profiles (cf. Figure 1). The liquor samples are closer to the fermented samples.  
386 However, differentiation on the level of country of origin is only revealed upon further analysis.  
387 We make a correlation network using the correlation matrix for cocoa samples, and show that  
388 systematic variation of a single parameter, namely correlation threshold, can be used to reveal  
389 grouping of cocoa samples on the basis of processing-stage, viz. unfermented, fermented and  
390 liquor, and country of origin. In the low and intermediate ranges of correlation threshold  
391 processing-stage sample type clusters are revealed, and in the higher range of correlation  
392 threshold the clustering of cocoa samples on the basis of country of origin is witnessed. We  
393 present our results both qualitatively (cf. Figure 2 and Figure 3) and quantitatively (cf. Figure  
394 4 and Figure 5). Besides a successful working approach, our work shows that differentiation  
395 of cocoa samples on the level of country of origin is on a more subtle level than their  
396 differentiation on the basis of processing-stage sample types.

397 It is worth comparing our approach to an often-used method in similar situation—the principal  
398 component analysis (PCA). PCA projects the samples into a lower dimensional space whose  
399 axes represent highest possible variation on the basis of the features in the dataset used in the  
400 analysis. Often it turns out that this analysis is also able to provide us a view in which samples  
401 with different classes well separated. However, there is no binding reason for it to be so, as  
402 PCA focuses on maximizing variation amongst the samples on the basis of their features and

403 not clustering them per se. Further, only truncated amount of information can be used to  
404 visualize the samples as we are limited to a maximum of three dimensions. On the other hand,  
405 in a correlation network information from all features (compounds used to calculate  
406 correlation) is present. Further, one is able to look at the structure of the network at the level  
407 of different amount of information by pruning the network thereby keeping low/high  
408 correlations as per need. In this sense, the approach of correlation networks is more  
409 sophisticated than that of PCA, omitting PCAs basic philosophy of data reduction.

410 Our study takes into consideration two factors on which cocoa samples may primarily differ:  
411 processing-stage and country of origin. However, it is worth noting these are not the only  
412 governing factors that affects similarity of cocoa samples. Many other factors such as variety  
413 of cocoa hybrid, soil, climate, terrain, harvesting season, farming practices etc. also have  
414 significant effects (Acierno et al., 2016; Adeniyi et al., 2019; Arévalo-Hernández et al., 2019;  
415 Ehiakpor et al., 2016; Kongor et al., 2016). It would be interesting to consider some of these  
416 factors in future works and see in what range of correlation threshold these effects start to  
417 matter, or can the inclusion of these additional factors give more clear modules of cocoa  
418 samples. Besides providing a new approach to study similarity in cocoa samples, our approach  
419 can be a compliment to the traditional approaches in this field.

420

## 421 **Acknowledgements**

422 We thank the whole COMETA team at Jacobs University which generated and gathered the  
423 LC-MS data over a period of five years, in particular Nina Böttcher and Britta Brehends for  
424 their excellent support in sample procurement, preparation and running experiments. SK is  
425 thankful to Johannes Falk and Piotr Nyczka for various stimulating and insightful discussions.

426 This work was funded by the COMETA Project, which is financially supported by Barry  
427 Callebaut AG.

## 428 **References**

429 Acierno, V., Yener, S., Alewijn, M., Biasioli, F., and van Ruth, S. (2016). Factors contributing  
430 to the variation in the volatile composition of chocolate: Botanical and geographical origins of  
431 the cocoa beans, and brand-related formulation and processing. *Food Research International*  
432 *84*, 86–95.

433 Acierno, V., Alewijn, M., Zomer, P., and van Ruth, S.M. (2018). Making cocoa origin  
434 traceable: Fingerprints of chocolates using Flow Infusion - Electro Spray Ionization - Mass  
435 Spectrometry. *Food Control* *85*, 245–252.

436 Adeniyi, S.A., de Clercq, W.P., and van Niekerk, A. (2019). Assessing the relationship between  
437 soil quality parameters of Nigerian alfisols and cocoa yield. *Agroforest Syst* *93*, 1235–1250.

438 Ahn, Y.-Y., Ahnert, S.E., Bagrow, J.P., and Barabási, A.-L. (2011). Flavor network and the  
439 principles of food pairing. *Sci Rep* *1*, 1–7.

440 Albert, R., and Barabási, A.-L. (2002). Statistical mechanics of complex networks. *Rev. Mod.*  
441 *Phys.* *74*, 47–97.

442 Arévalo-Hernández, C.O., da Conceição Pinto, F., de Souza Júnior, J.O., de Queiroz Paiva, A.,  
443 and Baligar, V.C. (2019). Variability and correlation of physical attributes of soils cultivated  
444 with cacao trees in two climate zones in Southern Bahia, Brazil. *Agroforest Syst* *93*, 793–802.

445 Barabási, A.-L., Gulbahce, N., and Loscalzo, J. (2011). Network medicine: a network-based  
446 approach to human disease. *Nature Reviews Genetics* *12*, 56–68.



- 447 Batushansky, A., Toubiana, D., and Fait, A. (2016). Correlation-Based Network Generation,  
448 Visualization, and Analysis as a Powerful Tool in Biological Studies: A Case Study in Cancer  
449 Cell Metabolism. *BioMed Research International*.
- 450 Becker, T., Beber, M.E., Windt, K., and Hütt, M.-T. (2012). The impact of network  
451 connectivity on performance in production logistic networks. *CIRP Journal of Manufacturing  
452 Science and Technology* 5, 309–318.
- 453 Bertoldi, D., Barbero, A., Camin, F., Caligiani, A., and Larcher, R. (2016). Multielemental  
454 fingerprinting and geographic traceability of *Theobroma cacao* beans and cocoa products. *Food  
455 Control* 65, 46–53.
- 456 Borgatti, S.P., Mehra, A., Brass, D.J., and Labianca, G. (2009). Network Analysis in the Social  
457 Sciences. *Science* 323, 892–895.
- 458 Caligiani, A., Palla, L., Acquotti, D., Marseglia, A., and Palla, G. (2014). Application of <sup>1</sup>H  
459 NMR for the characterisation of cocoa beans of different geographical origins and fermentation  
460 levels. *Food Chemistry* 157, 94–99.
- 461 Claussen, J.C., Skiecevičienė, J., Wang, J., Rausch, P., Karlsen, T.H., Lieb, W., Baines, J.F.,  
462 Franke, A., and Hütt, M.-T. (2017). Boolean analysis reveals systematic interactions among  
463 low-abundance species in the human gut microbiome. *PLOS Computational Biology* 13,  
464 e1005361.
- 465 Dogrusoz, U., Giral, E., Cetintas, A., Civril, A., and Demir, E. (2009). A Layout Algorithm for  
466 Undirected Compound Graphs. *Inf. Sci.* 179, 980–994.

- 467 D'Souza, R.N., Grimbs, S., Behrends, B., Bernaert, H., Ullrich, M.S., and Kuhnert, N. (2017).  
468 Origin-based polyphenolic fingerprinting of *Theobroma cacao* in unfermented and fermented  
469 beans. *Food Research International* 99, 550–559.
- 470 Ehiakpor, D.S., Danso-Abbeam, G., and Baah, J.E. (2016). Cocoa farmer's perception on  
471 climate variability and its effects on adaptation strategies in the Suaman district of western  
472 region, Ghana. *Cogent Food & Agriculture* 2, 1210557.
- 473 Fayeulle, N., Meudec, E., Boulet, J.C., Vallverdu-Queralt, A., Hue, C., Boulanger, R.,  
474 Cheynier, V., and Sommerer, N. (2019). Fast Discrimination of Chocolate Quality Based on  
475 Average-Mass-Spectra Fingerprints of Cocoa Polyphenols. *J. Agric. Food Chem.* 67, 2723–  
476 2731.
- 477 Grimbs, A., Klosik, D.F., Bornholdt, S., and Hütt, M.-T. (2019). A system-wide network  
478 reconstruction of gene regulation and metabolism in *Escherichia coli*. *PLOS Computational*  
479 *Biology* 15, e1006962.
- 480 Guehi, T.S., Zahouli, I.B., Ban-Koffi, L., Fae, M.A., and Nemlin, J.G. (2010). Performance of  
481 different drying methods and their effects on the chemical quality attributes of raw cocoa  
482 material. *International Journal of Food Science & Technology* 45, 1564–1571.
- 483 Hagberg, A.A., Schult, D.A., and Swart, P.J. (2008). Exploring Network Structure, Dynamics,  
484 and Function using NetworkX. In *Proceedings of the 7th Python in Science Conference*, p.
- 485 Hochberg, U., Degu, A., Toubiana, D., Gendler, T., Nikoloski, Z., Rachmilevitch, S., and Fait,  
486 A. (2013). Metabolite profiling and network analysis reveal coordinated changes in grapevine  
487 water stress response. *BMC Plant Biology* 13, 184.

- 488 Jeong, H., Tombor, B., Albert, R., Oltvai, Z.N., and Barabási, A.-L. (2000). The large-scale  
489 organization of metabolic networks. *Nature* *407*, 651–654.
- 490 Kamada, T., and Kawai, S. (1989). An algorithm for drawing general undirected graphs.  
491 *Information Processing Letters* *31*, 7–15.
- 492 Kongor, J.E., Hinneh, M., de Walle, D.V., Afoakwa, E.O., Boeckx, P., and Dewettinck, K.  
493 (2016). Factors influencing quality variation in cocoa (*Theobroma cacao*) bean flavour profile  
494 — A review. *Food Research International* *82*, 44–52.
- 495 Kuhnert, N., Dairpoosh, F., Yassin, G., Golon, A., and Jaiswal, R. (2013). What is under the  
496 hump? Mass spectrometry based analysis of complex mixtures in processed food – lessons  
497 from the characterisation of black tea thearubigins, coffee melanoidines and caramel. *Food*  
498 *Funct.* *4*, 1130–1147.
- 499 Kumar, S., and Deo, N. (2012). Correlation and network analysis of global financial indices.  
500 *Phys. Rev. E* *86*, 026101.
- 501 Kumar, S., Mahajan, S., and Jain, S. (2018). Feedbacks from the metabolic network to the  
502 genetic network reveal regulatory modules in *E. coli* and *B. subtilis*. *PLOS ONE* *13*, e0203311.
- 503 Kumari, N., Grimbs, A., D’Souza, R.N., Verma, S.K., Corno, M., Kuhnert, N., and Ullrich,  
504 M.S. (2018). Origin and varietal based proteomic and peptidomic fingerprinting of *Theobroma*  
505 *cacao* in non-fermented and fermented cocoa beans. *Food Research International* *111*, 137–  
506 147.
- 507 Lima, L.J.R., Almeida, M.H., Nout, M.J.R., and Zwietering, M.H. (2011). *Theobroma cacao*  
508 L., “The Food of the Gods”: Quality Determinants of Commercial Cocoa Beans, with Particular

- 509 Reference to the Impact of Fermentation. *Critical Reviews in Food Science and Nutrition* *51*,  
510 731–761.
- 511 Marseglia, A., Acquotti, D., Consonni, R., Cagliani, L.R., Palla, G., and Caligiani, A. (2016).  
512 HR MAS 1H NMR and chemometrics as useful tool to assess the geographical origin of cocoa  
513 beans – Comparison with HR 1H NMR. *Food Research International* *85*, 273–281.
- 514 McKinney, W. (2010). Data Structures for Statistical Computing in Python. In Proceedings of  
515 the 9th Python in Science Conference, S. van der Walt, and J. Millman, eds. pp. 51–56.
- 516 McKinney, W. (2011). pandas: a Foundational Python Library for Data Analysis and Statistics  
517 | R (Programming Language) | Database Index. In PyHPC 2011, p.
- 518 Megías-Pérez, R., Grimbs, S., D’Souza, R.N., Bernaert, H., and Kuhnert, N. (2018). Profiling,  
519 quantification and classification of cocoa beans based on chemometric analysis of  
520 carbohydrates using hydrophilic interaction liquid chromatography coupled to mass  
521 spectrometry. *Food Chemistry* *258*, 284–294.
- 522 Milev, B.P., Patras, M.A., Dittmar, T., Vrancken, G., and Kuhnert, N. (2014). Fourier  
523 transform ion cyclotron resonance mass spectrometrical analysis of raw fermented cocoa beans  
524 of Cameroon and Ivory Coast origin. *Food Research International* *64*, 958–961.
- 525 Namaki, A., Shirazi, A.H., Raei, R., and Jafari, G.R. (2011). Network analysis of a financial  
526 market based on genuine correlation and threshold method. *Physica A: Statistical Mechanics*  
527 *and Its Applications* *390*, 3835–3841.
- 528 Newman, M. (2003). The Structure and Function of Complex Networks. *SIAM Rev.* *45*, 167–  
529 256.

- 530 Oberrauter, L.-M., Januszewska, R., Schlich, P., and Majchrzak, D. (2018). Sensory evaluation  
531 of dark origin and non-origin chocolates applying Temporal Dominance of Sensations (TDS).  
532 Food Research International *111*, 39–49.
- 533 Oliveira, L.F., Braga, S.C.G.N., Augusto, F., Hashimoto, J.C., Efraim, P., and Poppi, R.J.  
534 (2016). Differentiation of cocoa nibs from distinct origins using comprehensive two-  
535 dimensional gas chromatography and multivariate analysis. Food Research International *90*,  
536 133–138.
- 537 Ozretic-Dosen, D., Skare, V., and Krupka, Z. (2007). Assessments of country of origin and  
538 brand cues in evaluating a Croatian, western and eastern European food product. Journal of  
539 Business Research *60*, 130–136.
- 540 Pluskal, T., Castillo, S., Villar-Briones, A., and Orešič, M. (2010). MZmine 2: Modular  
541 framework for processing, visualizing, and analyzing mass spectrometry-based molecular  
542 profile data. BMC Bioinformatics *11*, 395.
- 543 Shannon, P., Markiel, A., Ozier, O., Baliga, N.S., Wang, J.T., Ramage, D., Amin, N.,  
544 Schwikowski, B., and Ideker, T. (2003). Cytoscape: A Software Environment for Integrated  
545 Models of Biomolecular Interaction Networks. Genome Res. *13*, 2498–2504.
- 546 Sirbu, D., Grimbs, A., Corno, M., Ullrich, M.S., and Kuhnert, N. (2018). Variation of  
547 triacylglycerol profiles in unfermented and dried fermented cocoa beans of different origins.  
548 Food Research International *111*, 361–370.
- 549 Szklarczyk, D., Franceschini, A., Wyder, S., Forslund, K., Heller, D., Huerta-Cepas, J.,  
550 Simonovic, M., Roth, A., Santos, A., Tsafou, K.P., et al. (2015). STRING v10: protein–protein  
551 interaction networks, integrated over the tree of life. Nucleic Acids Res *43*, D447–D452.

552 Ursem, R., Tikunov, Y., Bovy, A., van Berloo, R., and van Eeuwijk, F. (2008). A correlation  
553 network approach to metabolic data analysis for tomato fruits. *Euphytica* *161*, 181.

554 Vázquez-Ovando, A., Molina-Freaner, F., Nuñez-Farfán, J., Betancur-Ancona, D., and  
555 Salvador-Figueroa, M. (2015). Classification of cacao beans (*Theobroma cacao* L.) of southern  
556 Mexico based on chemometric analysis with multivariate approach. *Eur Food Res Technol*  
557 *240*, 1117–1128.

558 Wang, L., Sun, X., Weiszmann, J., and Weckwerth, W. (2017). System-Level and Granger  
559 Network Analysis of Integrated Proteomic and Metabolomic Dynamics Identifies Key Points  
560 of Grape Berry Development at the Interface of Primary and Secondary Metabolism. *Front.*  
561 *Plant Sci.* *8*.

562 Wold, S., Esbensen, K., and Geladi, P. (1987). Principal component analysis. *Chemometrics*  
563 *and Intelligent Laboratory Systems* *2*, 37–52.

564

565

566